An elementary model of non-exponential decay. I. Description of model and comparison with other models

1994 J. Phys.: Condens. Matter 6 2881

(http://iopscience.iop.org/0953-8984/6/15/011)

J. Phys.: Condens. Matter 6 (1994) 2881–2892. Printed in the UK

An elementary model of non-exponential decay: I. Description of model and comparison with other models

P Erhart†, A M Portis‡, B Senning† and F Waldner†

† Physics Institute, University of Zürich, CH-8057 Zürich, Switzerland

‡ Department of Physics, University of California, Berkeley, CA 94720, USA

Received 7 July 1993, in final form 19 January 1994

Abstract. The motivation of this work is to search for an elementary common physical mechanism for the non-exponential decay observed in a large number of disparate phenomena. Probably the most elementary assumption is an initial Poissonian distribution of activation energies E with each fraction decaying independently according to an Arrhenius rate $r(E) \sim \exp(-E/T)$. Despite this drastic oversimplification, this elementary model will account for a large variety of observed shapes of decay, ranging from nearly exponential to power law and nearly logarithmic functions. The fundamental feature that governs the shape is the ratio $\bar{E}/T$, denoted $1/b$, of the mean $\bar{E}$ at temperature T. Analysing limited experimental data sets is also easy due to the closed form of the resulting normalized decay curves $g(b, \tau) = b\tau^{-b}\gamma(b, \tau)$, where $\tau = r_0 t$ is the time t normalized by the rate r_0. The incomplete gamma function $\gamma(b, \tau) = \int_0^\tau s^{b-1}e^{-s}\,ds$ is an important correction of the power law τ^{-b}.

In an alternative interpretation, this decay form $g(b, \tau)$ could also be considered as generated by a b-dependent form of an effective barrier energy $U_{\text{eff}}(g)$ increasing as a function of the decaying normalized observable g.

In this paper the forms $g(b, \tau)$ and $U_{\text{eff}}(g)$ are evaluated, displayed and compared with existing models. In a separate paper the widespread applicability of the form $g(b, \tau)$ will be demonstrated by interpreting various types of measured data using individual established temperature dependencies and by treating the 'ageing' or 'memory' effect.

1. Introduction

1.1. Measured decay in disordered materials

Non-exponential thermal relaxation of a non-equilibrium macroscopic observable $X(t)$ [1–9] is a widespread phenomenon in materials exhibiting some kind of disorder. Although the microscopic effects are very different and dependent upon the type of material, it is an intriguing fact that the decay curves are quite similar, and include decays close to exponential, power or logarithmic laws. Explaining the microscopic-scale physics [10–24] responsible for these experimental decay functions is a very complex task. Although there are some similarities, these theories have to treat in detail the specific effects for each material.

1.2. Generalizing models: the problem of temperature dependence

It is the aim of this paper to find a generalized model for non-exponential decay based on elementary physics.

At first glance, the temperature dependence should be part of every decay model. However, the temperature variation of non-exponential decay is different for granular

0953-8984/94/152881+12$19.50

superconductors, for metallic spin glasses, for the magnetic after-effect in alloys, and for the plastic elongation of a stretched copper wire.

In order to separate general from individual behaviour, a two-step procedure has been used. In a first step, generalized models interpret only single decay curves measured at a fixed temperature. In a second step, the individuality of the specific material will be considered. Already established temperature dependencies are incorporated for the specific material under investigation.

1.3. Early models using generating functions

In principle, non-exponential decay functions $x(t)$ are uniquely defined by two complementary generating functions: (i) a single effective rate $r_{\text{eff}}(x)$ varying with the decaying observable x, and (ii) an initial distribution $a_0(r)$ of relaxation rates r with each fraction decaying exponentially with constant rate r.

As long ago as 1937 Richter [25] introduced a broad distribution of relaxation rates. The resulting decay function is then a superposition of independent relaxations of the Arrhenius type. In order to enable a closed form for the resulting decay, he approximated the broad distribution by a box-type distribution. This model was applied to non-exponential decay of the magnetic after-effect.

In 1947 Kuhlmann [26] mentioned that the complementary method (i) of a single generating effective rate could also be used to describe non-exponential decay.

In 1948 Smith [27] explained the plastic elongation of stretched metals by assuming a flat distribution of activation energies. The resulting nearly logarithmic decay is again expressed in a closed form.

In 1989, Bourrous and Kronmüller [28] found a barrier distribution by fitting experimental data. For practical reasons, the number of fitting parameters (in principle infinite) was reduced by assuming an asymmetric Gaussian distribution. This model was applied to the magnetic after-effect in an amorphous alloy.

In 1989 Hagen and Griessen [13] assumed a distribution $m(E^*)$ of energy E^* for the pinning barriers in high-T_c superconductors. At that time, only the nearly logarithmic long-time fraction of the decay was well registered, which made it difficult to directly determine the distribution $m(E^*)$ from a measurement at fixed T. Instead, these authors used an established temperature dependence for $E(T)$ together with the full temperature dependence of the decay at long times and found by an inversion scheme the distribution $m(E^*)$.

In 1993 Theuss [29] compared, for the same data of layered type-II superconductors, the inversion scheme of Hagen and Griessen [13] with the modified method of Bourrous and Kronmüller [28]. The distribution is approximated by many box-type distributions, using the integral evaluated by Richter [25] for each box. In addition, the data at four different temperatures were combined for the determination of one distribution.

1.4. Proposing an elementary initial distribution

Although the papers described in the previous section show that non-exponential decay can be related to an underlying distribution function, there are two problems. First, the evaluation of this function for limited experimental data is difficult due to the, in principle infinite, number of fitting parameters. Second, the distribution found by inversion is a very helpful type of *presentation* of the observed data rather than their interpretation or explanation. Therefore, it is advisable to expand the generating method from the formal box-type of Richter [25] to distributions based on elementary stochastic arguments in order to suggest an *explanation* of the data.

The simplest approach of a Poissonian distribution was able to interpret a large number of decay data with only a small number of fitting parameters. Only in the cases of bad fits is the distribution modified, again using a physical argument that the low-energy part has already decayed at the 'initial' time of the decay. Such distributions coincide with the results of Hagen and Griessen [13] found by inversion. Such an 'elementary decay model' (EDM) was sketched [30] in 1991 and will be presented here in more detail.

The decay functions of the EDM will then be compared with predictions [10–23] of other models and with a Monte Carlo simulation [11] of the Sherrington–Kirkpatrick model.

In the following paper, the EDM will be applied to various experiments. An important application is the description of the 'ageing' or 'memory' effect. A discussion will show that the ageing effect is a consequence of specific decay curves, and not directly related to spin glass behaviour.

2. Introducing the 'elementary decay model' (EDM)

2.1. Generalizing thermal activation

It seems sufficient to consider only the decay after a sudden change of an external parameter since the response to a continuous change has been described elsewhere [30].

Suppose the non-equilibrium observable $X(t)$ starts after a step of an external parameter occurring at $t = 0$ with the initial value X_0. Describing by $X(t)$ only the non-equilibrium part, $X(t)$ will decay to zero. Thus the normalized decay function $x(t) = X(t)/X_0$ starts at one and decays to zero.

The main common feature of the decay in the large variety of disordered materials is that the decay $X(t)$ at a fixed temperature T is caused by thermal activation of energy E. The basic assumption is, therefore, an Arrhenius type of the decay rate $r(E') = -(1/X)\,dX/dt = -(1/x)\,dx/dt$ proportional to $\exp(-E')$ where $E' = E/T$ is the normalized activation energy. Three possible interpretations of non-exponential decay will be considered.

(i) The energy E' is assumed to change during the process of relaxation, to be described by $E'(t)$ or, implicitly, by an effective activation energy $U'_{\mathrm{eff}}(x)$ as a function of the normalized decaying observable x, with $r_{\mathrm{eff}}(x) \propto \exp\{-U'^{(r)}_{\mathrm{eff}}(x)\}$†. This description implies a uniform behaviour over the sample.

Although the transform $x(t) \rightarrow r_{\mathrm{eff}}(x)$ is straightforward, the inverse transform $r_{\mathrm{eff}} \rightarrow t(x) \rightarrow x(t)$ cannot always be performed in closed form.

(ii) A non-uniform behaviour would result in a distribution $f(E')$ of energies $E' = E/T$. If these energies E' are constant during the process of relaxation, the superposition of the resulting exponential decay functions would already yield non-exponential decay functions, without the need to assume that these energies are of the changing $U'_{\mathrm{eff}}(x)$ type, as demonstrated by various authors [13, 25, 27–29], and also discussed by Palmer and co-workers [31]. In the limit of a continuous rate $r = r_0 \exp(-E')$ with the maximal value r_0 for $E' = 0$‡ the decay $x(t)$ is expressed as [31]

$$x(a_0, \tau) = \int_0^1 a_0(\check{r}) \exp(-\check{r}\tau)\, d\check{r} \tag{1}$$

† Note that some microscopic models [11, 15–20] relate rather the normalized *slope* $s_{\mathrm{eff}}(x) = -dx/dt = -(1/X_0)\,dX/dt$ instead of the *rate* $r_{\mathrm{eff}}(x) = (1/x)\,s_{\mathrm{eff}}(x)$ to a thermally activated normalized energy $U'_{\mathrm{eff}} = U_{\mathrm{eff}}/T$ by assuming $s_{\mathrm{eff}}(x) \propto \exp[-U'^{(s)}_{\mathrm{eff}}(x)]$ instead of the previous $r_{\mathrm{eff}}(x) \propto \exp[-U'^{(r)}_{\mathrm{eff}}(x)]$.

‡ Note that an additional arbitrary fixed energy E'_0 could be added to E' by using $r/r_{00} = \exp[-(E' + E'_0)]$ after setting $r_0 = r_{00} \exp E'_0$.

where a normalized rate $\check{r} = r/r_0 = \exp(-E')$ and a normalized time $\tau = r_0 t$ has been used. The decay is then governed by the generating initial distribution function $a_0(\check{r})$ with $\check{r}$ ranging between zero and one, normalized to $\int_0^1 a_0(\check{r})\mathrm{d}\check{r} = 1$. Note that the transform $a_0(\check{r}) \rightarrow x(t)$ corresponds to the Laplace transform†. Therefore, the inverse transform $x(t) \rightarrow a_0(\check{r})$ might be mathematically involved.

(iii) In reality, probably a combination of (i) and (ii) occurs, which cannot be treated easily in closed form.

As mentioned by Kuhlmann [26] in 1947, an important fact is that, from knowledge of decay curves of only one macroscopic observable $x(t)$ alone, it is impossible to discriminate between these various possibilities.

2.2. *An elementary initial distribution results in a closed form*

Probably the most elementary form for a stochastic distribution is an *exponential* distribution $f_0(E') \propto \exp(-E/\bar{E})$ corresponding to the assumption of a random distribution of activation energies E in the limit of a continuous Poissonian with mean value $\bar{E}$. This assumption seems rather artificial, but it could be considered as a limiting case, and it will interpret many of the observed features. This distribution has the advantage of being governed by only *one* parameter $b = T/\bar{E}$ and the resulting decay function can be evaluated in closed form. Using the normalized notation $E' = E/T$ equation (1) yields for the normalized decay function $g(b, \tau)$ an integral over a time-dependent distribution $f(E', \tau)$ as a function of the normalized time $\tau = r_0 t$

$$g(b, \tau) = \int_{E'=0}^{\infty} f(E', \tau)\,\mathrm{d}E' \tag{2}$$

$$f(E', \tau) = f_0(E')\exp[-\exp(-E')\tau] \tag{3}$$

$$f_0(E') = b\exp(-bE') = (T/\bar{E})\exp(-E/\bar{E}). \tag{4}$$

This normalized initial distribution $f_0(E') = b\exp(-bE')$ is characterized by the ratio $\bar{E}/T = 1/b$. Every fraction between E' and $E' + \mathrm{d}E'$ decays independently with its characteristic rate $\check{r}(E') = \exp(-E')$.

To evaluate the resulting decay in closed form, it is convenient to transform to (1) with $-E' = \ln \check{r}$, with the details given in appendix A. The resulting form for the decay consists of a product of b with the power law τ^{-b} and with an integral known as the incomplete gamma function $\gamma(b, \tau) = \int_0^\tau s^{b-1}\mathrm{e}^{-s}\,\mathrm{d}s$ [32], which is incorporated in computer libraries [33]

$$g(b, \tau) = b\tau^{-b}\int_0^\tau s^{b-1}\mathrm{e}^{-s}\,\mathrm{d}s = b\tau^{-b}\gamma(b, \tau). \tag{5}$$

The single parameter $b = T/\bar{E}$ determines the type of decay: nearly logarithmic for $b \ll 1$, but with the correct values one and zero for $t = 0$ and $t \rightarrow \infty$, respectively, then for intermediate values of b close to power law, but starting at one, and approximating an exponential behaviour for $b \gg 1$. Figure 1 displays these functions in a linear plot in order to show both the initial and limiting behaviour, and figures 2 and 3 plot the functions in various ways in order to show the similarities to simpler functions.

In the next section a variation of the initial distribution will be introduced which affects the short-time behaviour. An example for varying the long-time behaviour will be described in the following paper, where a Kohlrausch form is approximated by a distribution which has a Gaussian form at an intermediate time.

† Equation (1) corresponds to the Laplace transform $\bar{y}(p) = \int_0^\infty \exp(-pt)y(t)\,\mathrm{d}t$ for $x(\tau) \rightarrow \bar{y}(p)$ and $a_0(\check{r}) \rightarrow y(t)$ with $y(t > 1) = 0$.

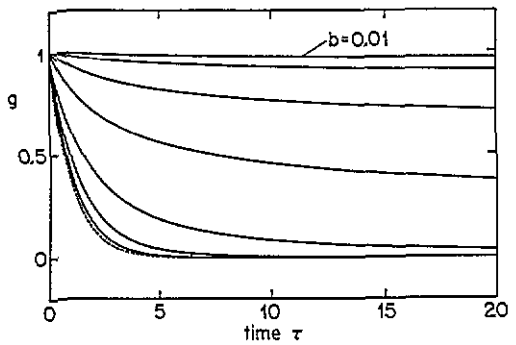

Figure 1. Normalized decay function $g(b, \tau) = X(\tau)/X_0$ against normalized time $\tau = r_0 t$ with global rate r_0, displayed for the values $b = kT/\bar{E}$ (from top) 0.01, 0.03, 0.1, 0.3, 1, 3, 10. The broken curve corresponds to $\exp(-\tau)$.

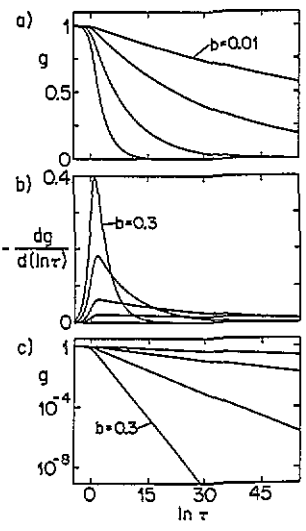

Figure 2. Decay function $g(b, \tau)$ for $b = 0.01$, 0.03, 0.1, 0.3. (*a*) $g(b, \tau)$ against $\ln \tau$; (*b*) derivative $-\mathrm{d}g/\mathrm{d}(\ln \tau)$ against $\ln \tau$; (*c*) regions close the power law $g \propto \tau^{-b}$ are shown in a ln–ln plot: $\ln g(b, \tau)$ against $\ln \tau$.

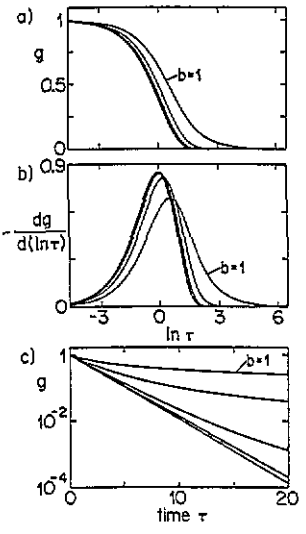

Figure 3. Similar to figure 2, but for b values (*a*), (*b*) $b = 1$, 3, 10 and (broken curve) $\exp(-\tau)$; except (*c*) regions close to exponential $\exp(-\tau)$ are shown in a ln–linear plot $\ln g(b, \tau)$ against τ for $b = 1$, 3, 10, 30, and (broken curve) $\exp(-\tau)$.

2.3. Variation of the initial distribution for short times

In figure 4 the function f/b is shown for different times τ. Clearly, there is a peak at $E'_{\mathrm{peak}}(\tau) = \ln(\tau/b)$ for $\tau/b > 1$, thus $E'_{\mathrm{peak}}(\tau)$ increases with the *logarithm* of the time τ.

This indicates that the EDM could also easily interpret initial conditions starting at $\tau^* = 0$ with a distribution exhibiting a peak at a finite energy $E'_{0-\mathrm{peak}}(\tau^* = 0) = \ln(\tau_{\mathrm{in}}/b)$, to be fixed by the parameters $b = 1/\bar{E}'$ and a fictive initial time τ_{in} or $E'_{0-\mathrm{peak}}$. This new normalized decay function $g^{(2)}(b, \tau_{\mathrm{in}}; \tau^*)$ starts at the new time $\tau^* = 0$ with $\tau = \tau^* + \tau_{\mathrm{in}}$ by defining the two-parameter decay function $g^{(2)}$ of the EDM:

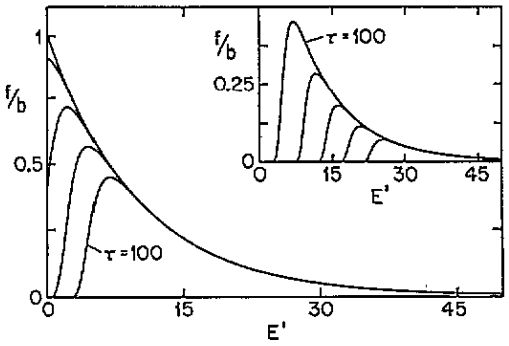

Figure 4. Distribution function $f(E', \tau)/b$ against $E' = E/T$ of (3) for $b = 0.1$, displayed at the normalized times $\tau = 0, 0.1, 1, 10, 100$. Inset: $\tau = 10^2, 10^4, 10^6, 10^8, 10^{10}$. Note that the distribution decays rapidly for small values of E' resulting in a peak at E'_{peak} which moves to higher energies, thus the *average* energy of the distribution $f(E', \tau)$ increases in time. The integral of these curves correspond to the decay function $g(b, \tau)$.

$$g^{(2)}(b, \tau_{\text{in}}; \tau^*) = g^{(2)}(b, E'_{0-\text{peak}}; \tau^*) = \frac{g(b, \tau = \tau^* + \tau_{\text{in}})}{g(b, \tau_{\text{in}})|_{\tau^*=0}}. \tag{6}$$

Only the short-time behaviour is strongly affected by this variation of the initial condition.

2.4. Universal distributions for larger times

The shapes of f/b in figure 4 for different times seem to be the same, only with decreasing amplitudes. Indeed, this behaviour is found for $\tau/b > 1$ by shifting the E' axis for $f(E', \tau)$ of (3), using $E'' = E' - E'_{\text{peak}}$, resulting in an integral over a function $u(b, E'')$ independent of τ, scaled by a factor $(\tau/b)^{-b}$, and starting at $-E'_{\text{peak}}(\tau) = -\ln(\tau/b)$:

$$g(b, \tau) = (\tau/b)^{-b} \int_{-\ln(\tau/b)}^{\infty} u(b, E'')\, \mathrm{d}E'' \qquad \tau/b > 1 \tag{7}$$

$$u(b, E'') = b \exp\{-b[E'' + \exp(-E'')]\}. \tag{8}$$

Note that the resulting functions $u(b, E'')$ of (8), as shown in figure 5, are shifted logarithmically in time along the E' axis, while their magnitude is decreases according to the power law $(\tau/b)^{-b}$ for $\tau/b > 1$. However, their shape is universal for a fixed value of b (see the inset of figure 4). Moreover, figure 5 shows that $u(b, E'')$ drops rapidly on the left-hand side such that, for long enough times $\tau/b \gg 1$, the integral in (7) is nearly constant, resulting in $g(b, \tau) \propto (\tau/b)^{-b}$, which contains a regime close to $\propto -b \ln \tau$ for $b \ll 1$, but also includes appropriate 'crossover' regions.

Furthermore, figure 4 indicates that despite the extreme assumption of a wide non-interacting distribution, at each time a 'characteristic' energy of the order of $E'_{\text{peak}}(\tau) = \ln \tau/b$ could be determined, which will be the relevant energy for the decay around that time τ since, to a good approximation, the activation at smaller energies is already decayed and the activation at much higher energies has not started to decay.

Since most existing models [11, 15–20] are based on the selection of a single 'characteristic' energy increasing in time, thus increasing with decreasing observable x, in the next section we treat the EDM accordingly.

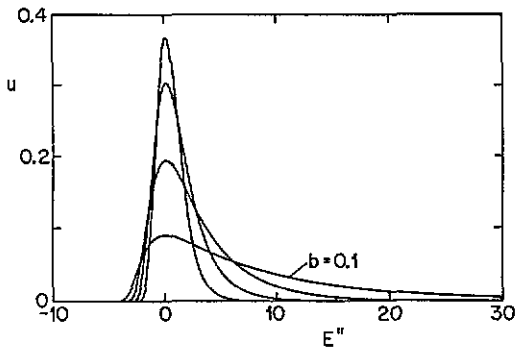

Figure 5. Distribution function $u(b, E'')$ of (8) against $E'' = E' - E'_{peak}$ for $b = 0.1, 0.25, 0.5, 1$, corresponding to $f(b, \tau)$ for $\tau/b > 1$, but shifted by $E'_{peak} = \ln(\tau/b)$.

2.5. The EDM interpreted by a single variable energy U_{eff}

Although the EDM has been constructed by a distribution of energies, E, constant in time, it could also be considered as governed by a single but variable energy $U_{\mathrm{eff}}(x)$ given as a function of the normalized observable x. Since the EDM has the advantage of yielding a closed form for $x(\tau) = g(b, \tau)$, see (5), the derivative can also be expressed in closed form:

$$-\frac{\mathrm{d}g}{\mathrm{d}\tau} = \check{s}_{\mathrm{eff}}(g) = g\check{r}_{\mathrm{eff}}(g) = \frac{b}{\tau}\left(1 - \frac{\exp(-\tau)}{g(\tau)}\right)g(\tau) \tag{9}$$

where $\check{s} = s/r_0$ and $\check{r} = r/r_0$ are defined for derivatives with respect to $\tau = r_0 t$ instead of t. These effective energies can be evaluated with τ as an implicit variable:

$$\frac{U^{(r)}_{\mathrm{eff}}}{T} = U'^{(r)}_{\mathrm{eff}}[g(\tau)] = -\ln\left[\frac{b}{\tau}\left(1 - \frac{\exp(-\tau)}{g(\tau)}\right)\right] \tag{10}$$

and obviously† $U'^{(s)}_{\mathrm{eff}} = U'^{(r)}_{\mathrm{eff}} + \ln(1/g)$.

These functions will be displayed and discussed in the next section.

3. Comparison of the EDM with other models

3.1. Connecting $dg/d\tau$ of the EDM with I–V curves in superconductors

Before discussing the functions related to $\mathrm{d}g/\mathrm{d}\tau$, such as $\check{s}_{\mathrm{eff}}$ and $U'^{(s)}_{\mathrm{eff}}$, it seems helpful to point to a further interpretation of $\check{s}_{\mathrm{eff}}$, although it can only be applied to superconductors. In a superconductor subjected to a step in the applied magnetic field, the decaying normalized observable $x(t)$ might be the excess magnetization which is proportional to the normalized shielding current density $\check{J} = J/J_c = x$. Therefore, the decay $x(\tau)$ might be related by

$$-\frac{\mathrm{d}x}{\mathrm{d}\tau} = \check{s}_{\mathrm{eff}}(x) = x\check{r}_{\mathrm{eff}}(x) \propto E(\check{J}) = \check{J}\rho(\check{J}) \tag{11}$$

† Note that, as already mentioned, some microscopic models [11, 15–20] relate rather the normalized *slope* $s_{\mathrm{eff}}(x) = -\mathrm{d}x/\mathrm{d}t = -(1/X_0)\,\mathrm{d}X/\mathrm{d}t$ instead of the *rate* $r_{\mathrm{eff}}(x) = (1/x)\,s_{\mathrm{eff}}(x)$ to a thermally activated normalized energy $U'_{\mathrm{eff}} = U_{\mathrm{eff}}/T$ by assuming $s_{\mathrm{eff}}(x) \propto \exp[-U'^{(s)}_{\mathrm{eff}}(x)]$ instead of the previous $r_{\mathrm{eff}}(x) \propto \exp[-U'^{(r)}_{\mathrm{eff}}(x)]$.

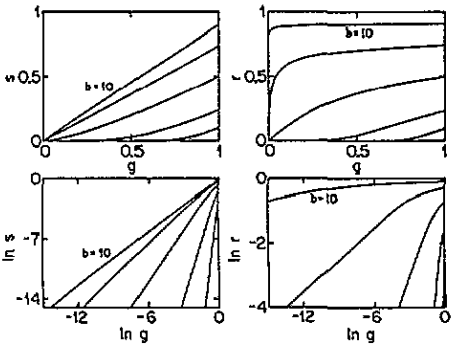

Figure 6. The EDM functions of (11). Left: $s = \check{s}_{\rm eff}(g)$. Right: $r = \check{r}_{\rm eff}(g)$ against decay value g. Both are linear (top) and ln–ln (bottom) plots for the values 0.1, 0.3, 1, 3, 10 of the parameter b.

with measurements of I–V current–voltage characteristics which yield the electric field $E(\check{J})$ and the resistivity $\rho(\check{J})$ as a function of an externally driven normalized current density $\check{J} = g$ when interpreted by the normalized g of the EDM.

In figure 6 the EDM functions $\check{s}_{\rm eff}(g)$ (left) and $\check{r}_{\rm eff}(g)$ (right) are displayed both in linear (top) and log–log (bottom) plots for the values 0.1, 0.3, 1, 3, 10 of the parameter b which determines the shape.

3.2. A peculiar phase transition typical for a spin glass

Excluding $\check{J} \approx 1$, the EDM result for $g(b, \tau)$ is well approximated by a power law $\propto \tau^{-b}$, yielding $\check{s}_{\rm eff} \propto g^{\delta}$ with an exponent $\delta = 1/b + 1$, and $\check{r}_{\rm eff} \propto g^{(1/b)} = g^{(\check{E}/T)}$. Therefore, in terms of I–V characteristics, the *limiting resistivity* $\rho_{\rm lim} = \lim_{\check{J}\to 0}[E(\check{J})/\check{J}]$ is zero for all values of b, except for $b \to \infty$ corresponding to $T \to T_c$.

The EDM, combined with a temperature dependence of $\check{E}(T)/T = 1/b$ established for superconductors, predicts zero limiting resistivity for all temperatures below T_c. However, for $T > T_{b=1}$ a very small $\check{J} \ll 1$ creates a rather large resistivity, because the limiting slope $[{\rm d}\rho/{\rm d}\check{J}]_{\lim \check{J}\to 0}$ is infinite. A peculiar phase transition occurs at $T_{b=1}$: the *limiting slope* $[{\rm d}\rho/{\rm d}\check{J}]_{\lim \check{J}\to 0}$ undergoes a sharp transition from infinity to zero, see figure 6 (top right). This continuous sharp transition is rounded by non-zero current density $\check{J} > 0$. For small $\check{J}$ there is a 'crossover' type of transition between measurable to negligible resistance around the value $1/b = \check{E}/T \approx 1$, dependent upon the value chosen for that small $\check{J}$; see again figure 6 (top right). Hence this peculiar phase transition of a *slope*, rounded by non-zero currents, is similar to the cusp-type feature of the susceptibility of a metallic spin glass, with the cusp rounded by non-zero magnetic fields.

3.3. Comparing the resistivity of the EDM with the scaling theory

The peculiar phase transition at $T_{b=1}$ of the resistivity of the EDM has qualitatively many features of the continuous-vortex–glass phase transition at the finite temperature $T_{\rm vg}$ in superconductors, as reviewed by Huse and co-workers [34] based on scaling theory (ST), although they differ quantitatively.

The linear resistivity of the ST, which undergoes a sharp transition to zero, is defined as the limit $\rho_1 \equiv \lim_{J\to 0}\{E/J\}$. While the ST discriminates between 'linear' and 'non-linear' resistivity $\rho \equiv E/J$, the EDM uses only $\rho(J) = E/J$, which implies the non-linear

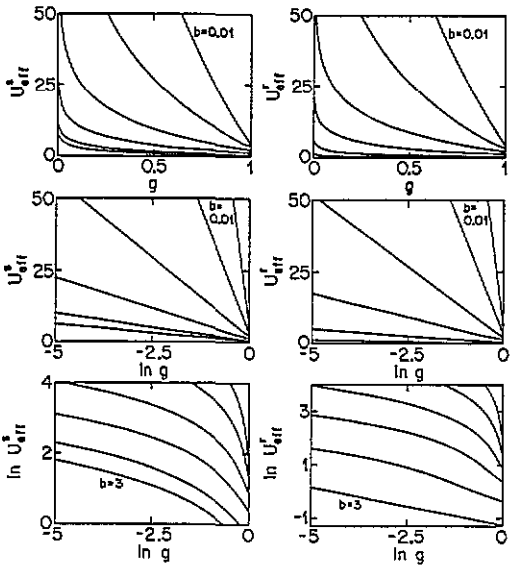

Figure 7. Effective normalized energies $U^s_{\rm eff} = U^{(s)}_{\rm eff}/T$ (left), and $U^r_{\rm eff}$ (right) against decay value g in linear–linear (top), linear–ln (centre) and ln–ln (bottom) plots for the values 0.01, 0.03, 0.1, 0.3, 1, 3 of the parameter b.

resistivity below $T_{\rm vg}$ of the ST. Both models predict a power law for $\rho(J)$ around the phase transition for finite $J > 0$. In both models a sharp phase transition occurs only in the limit of vanishing current density $J \to 0$. In the ST the limiting resistivity changes from a finite value to zero. In the EDM the limiting resistivity remains zero, but the limiting *slope* $[{\rm d}\rho/{\rm d}J]_{\lim J\to 0}$ changes from ∞ to zero. (Note that the limiting slope of the non-linear resistivity of the ST is also zero below $T_{\rm vg}$.) For finite current density $J > 0$ the resistivity changes strongly around the transition temperature to very small values but remains, in principle, finite below the transition in both models.

Whereas the ST uses the scaling ansatz together with at least pinning at random positions or, according to Nattermann [15], also 'pinning at arbitrary high energy barriers', the EDM only assumes a distribution of pinning energies combined with an established temperature dependence of the mean pinning energy $\bar{E}(T)$, which is already sufficient to include indirectly a peculiar phase transition of the spin glass type.

3.4. Comparing $U_{\rm eff}$ of the EDM with other theories

Returning to the general case, which includes spin glasses, the effective activation energies $U^{\prime(s)}_{\rm eff}(g)$ (left) and $U^{\prime(r)}_{\rm eff}(g)$ (right) are displayed in figure 7 in linear–linear (top), linear-$U_{\rm eff}$–ln g (centre) and ln–ln (bottom) plots for the parameter values $b = 0.01, 0.03, 0.1, 0.3, 1, 3$.

The linear–linear plot of figure 7 (top left) shows that $U^{\prime(s)}_{\rm eff}$ approximates the Anderson function $\propto 1 - \check{J}$ for $b \to 0$. Furthermore, the linear-$U'_{\rm eff}$–ln g plots of figure 7 (centre) indicate that these functions are close to $\propto \delta \ln(1/g)$ with $\delta_s = 1/b + 1$ and $\delta_r = 1/b$ for $U'^{(s)}$ and $U'^{(r)}$, respectively, as evaluated with the approximation $g \propto \tau^{-b}$, with deviations visible around $g \approx 1$. Therefore, the ln–ln plots of $U'_{\rm eff}(g)$ in figure 7 (bottom) show curves with continuously changing slopes. Thus if $U'_{\rm eff}(g)$ is interpreted by a power law $\propto (1/\check{J})^{\mu}$, as proposed by various authors [15, 16, 18], a continuous 'crossover' of the value of μ would result, although a fit with a power law would look reasonable within smaller intervals of $\check{J}$. However, the EDM coincides with the exact solution $U_{\rm eff} = U_0 \ln(1/\check{J})$ found by Blatter [17, 21] when the vortex motion is controlled by intrinsic pinning in a layered system for a field parallel to the layers. This logarithmic dependence has been applied to find an exact solution for flux creep in a slab by Vinokur and co-workers [22].

3.5. Comparing the EDM with decay forms of other models

How well do the decay curves $g(b, \tau)$, proposed by the EDM, describe decay curves proposed by other models? Note that there is only one parameter, b, that determines the shape. For the prediction of *logarithmic decay* this could be tested in figures 2(*a*) and (*b*) where ln–linear plots and plots of the derivatives with respect to $\ln \tau$ are shown. Clearly, this is the case for small values of b.

The prediction of a *power law* can be tested in figure 2(*c*). It is indicated by nearly straight lines in the log–log plot for a wide range of values of b.

3.6. Comparison of the EDM with the Sherrington–Kirkpatrick model

Fisher and co-workers [11] have performed Monte Carlo simulations of the Sherrington–Kirkpatrick (SK) model in order to estimate the dynamic exponent α of their scaling hypothesis $q_0(t) \propto (\ln t)^{-\alpha}$ valid for large times t. Indeed, their simulation data [11] plotted in a $\log q_0$ against $\log(\log t)$ plot, see figure 8, show a constant value for the exponent α for large t, as predicted.

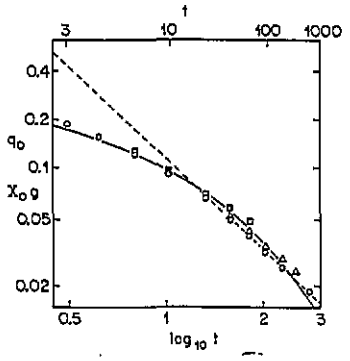

Figure 8. Monte Carlo simulation of [11] of the Sherrington–Kirkpatrick model: time dependence of the remanent magnetization $m(t) = q_0(t)$ for N spins (N = 50, 160, 512 for squares, triangles, circles, respectively). Broken curve: exponent $\mu = 1.75$ of $q_0 \propto (\ln t)^{-\mu}$. Full curve: $X_0 g(b, r_0 t)$ of the EDM with $X_0 = 0.707$, $b = 0.43$, $r_0 = 6.1$.

When the same data are fitted by the EDM based on the hypothesis of an independently decaying Poissonian initial distribution of activation energies, the resulting curved function of figure 8 fits well the data points of the simulation of the SK model [11] in the whole time interval.

4. Concluding remarks

In summary, the 'elementary decay model' (EDM) presented here has been constructed to interpret non-exponential decay regimes observed in spin glasses and superconductors by an elementary stochastic assumption for an initial distribution of activation energies. The resulting decay functions are expressed in closed form and cover the entire decay from the starting value to the final value of the observable without the need to define 'epochs' connected by 'crossover' regions. Furthermore, the magnitude of the ratio $\bar{E}/T$ of the initial distribution governs the type of decay, ranging continuously from exponential over power to logarithmic law without the need to define 'changeover' regimes between these specific decay forms.

The main result of the application of the EDM to measurements as described in the following paper is the fact that the elementary hypothesis of a stochastic initial distribution is sufficient to interpret a large variety of data when established temperature dependencies for $\bar{E}(T)$ are used.

Acknowledgments

The authors would like to thank M Brodmann, J E Drumheller, C W Hagen, K A Müller, T Nattermann, C Rossel, R Verfürth and M Warden for helpful comments. This work has been supported by the Swiss National Science Foundation.

Appendix. Evaluation of the closed form of the EDM

The exponential initial distribution $f_0(E')\,dE' = b\exp(-bE')\,dE'$ of (2) with the notation $b = T/\bar{E}$ and $E' = E/T$ is transformed to the form of (5) by the relation $-E' = \ln\check{r}$ yielding $a_0(\check{r})\,d\check{r} = -b\check{r}^{(b-1)}\,d\check{r}$ where $\check{r} = r/r_0$. The resulting decay $x(\tau) = g(b,\tau)$ is then a function of b and the normalized time $\tau = r_0 t$. For $b = 1$ the integral in (1) has the solution $g(1,\tau) = [1-\exp(-\tau)]/\tau$. For $(b \neq 1)$ this form has the advantage that the integral in (1) can either be solved when transformed into a series of integrable terms†

$$g(b,\tau) = b\int_0^1 \check{r}^{(b-1)}\exp(-\check{r}\tau)\,d\check{r} = b\sum_{n=0}^{\infty}\int_0^1 \frac{(-1)^n\tau^n\check{r}^{(b-1+n)}}{n!}\,d\check{r} \qquad (A1)$$

$$= b\sum_{n=0}^{\infty}\frac{(-1)^n\tau^n}{(b+n)n!} \qquad (A2)$$

or the integral can be transformed by the substitution $s = \check{r}\tau$ into a product of b with the power law τ^{-b} and with an integral known as the incomplete gamma function $\gamma(b,\tau) = \int_0^\tau s^{b-1}e^{-s}\,ds$ [32]

$$g(b,\tau) = b\tau^{-b}\int_0^\tau s^{b-1}e^{-s}\,ds = b\tau^{-b}\gamma(b,\tau). \qquad (A3)$$

References

[1] Binder K and Young A P 1986 *Rev. Mod. Phys.* **58** 801
[2] Müller K M, Takashige M and Bednorz J G 1987 *Phys. Rev. Lett.* **58** 1143
[3] Svedlindh P, Granberg P, Nordblad P, Lundgren L and Chem H S 1987 *Phys. Rev.* B **35** 268
[4] Lundgren L 1988 *J. Physique* **49** C8 1001
[5] Morgenstern I 1990 *Earlier and Recent Aspects of Superconductivity* ed J G Bednorz and K A Müller (Berlin: Springer) p 240
[6] Mota A C, Pollini A, Juri G, Visani P and Hilti B 1990 *Physica* **168A** 298
[7] Svedlindh P, Niskanen K, Norling P, Nordblad P, Lundgren L, Rossel C, Sergent M, Chevrel R and Potel M 1991 *Phys. Rev.* B **43** 2735
[8] Svedlindh P, Rossel C, Niskanen K, Norling P, Nordblad P, Lundgren L and Chandrashekhar G V 1991 *Physica* **176C** 336
[9] Chikumoto N, Koncykowski M, Motohira N, and Malozemoff A P 1992 *Phys. Rev. Lett.* **69** 1260
[10] Anderson P W 1962 *Phys. Rev. Lett.* **9** 309
[11] Fisher D S, Huse D A 1988 *Phys. Rev.* B **38** 373
[12] Rossel C, Maeno Y and Morgenstern I 1989 *Phys. Rev. Lett.* **62** 681

† The numerical evaluation of the series in (A2) is problematic for large τ. It can be replaced by the numerical integration of (A1) or (2)–(4) with adjusted variable integral steps. For $\tau/b > 1$, equations (7) and (8) might be more favourable.

Rossel C 1990 *Relaxation in Complex Systems and Related Topics (NATO ASI B Phys.* 222) ed I A Campbell and C Giovannella (New York: Plenum) pp 105–12
[13] Hagen C W and Giessen R 1989 *Phys. Rev. Lett.* **62** 2857
[14] Ferrari M J, Johnson M, Wellstood F C, Clarke J, Mitzi D, Rosenthal P A, Eom C B, Geballe T H, Kapitulnik A and Beasley M R 1990 *Phys. Rev. Lett.* **64** 72
[15] Nattermann T 1990 *Phys. Rev. Lett.* **64** 2454
[16] Feigel'man V M, Geshkenbein V B and Larkin A I 1990 *Physica* **167C** 177
[17] Blatter G, Ivlev B I and Rhyner 1990 *Eidgenössische Technische Hochschule Zürich report*
[18] Fisher D S, Fisher M P A and Huse D A 1991 *Phys. Rev.* B **43** 130
[19] Malozemoff A P 1991 *Physica* **185–9C** 264
[20] Brandt E H 1991 *Physica* **185–9C** 270
[21] Vinokur V V, Blatter G, Feigel'man M V, Geshkenbein V B and Larkin A I 1991 *Physica* 185-9C 276
[22] Vinokur V V, Feigel'man M V, Geshkenbein V B *Phys. Rev. Lett.* **67** 915
[23] Kes P H 1991 *Physica* **185–9C** 288
[24] Sibani P and Hoffmann K H 1989 *Phys. Rev. Lett.* **63** 2853
[25] Richter G 1937 *Ann. Phys.* **29** 605; 1938 *Ann. Phys.* **32** 683
[26] Kuhlmann D 1947 *Z. Phys.* **124** 468
[27] Smith C L 1948 *Proc. Phys. Soc.* **61** 14
[28] Bouorrous M and Kronmüller H 1989 *Phys. Stat. Sol. (a)* **113** 169, 383
[29] Theuss H 1993 *Physica* **208C** 155
[30] Erhart P, Senning B, Mini S, Fransioli L, Waldner F, Drumheller J E, Portis A M, Kaldis E and Rusiecki S 1991 *Physica* **185-9C** 2233
Erhart P, Drumheller J E, Portis A M, Senning B, Mini S, Fransioli L, Kaldis E, Rusiecki S and Waldner F 1992 *J. Magn. Magn. Mater.* **104–7** 487
[31] Palmer R G, Stein D L, Abrahams E and Anderson P W 1984 *Phys. Rev. Lett.* **53** 958
[32] Abramowitz M and Stegun A I 1968 *Handbook of Mathematical Functions* (New York: Dover) pp 260–2
[33] CERN Program Library, subroutine no. C305 for $\Gamma(b)$; no. G106 for $P(b, \tau)$; to be combined to $\gamma(b, \tau) = \Gamma(b) \cdot P(b, \tau)$.
[34] Huse D A, Fisher M P A, and Fisher D S 1992 *Nature* **358** 553